Development 138, 4535-4544 (2011) doi:10.1242/dev.071266

Renal collecting system growth and function depend upon embryonic γ1 laminin expression

Dong-Hua Yang[1,*], Karen K. McKee[1], Zu-Lin Chen[2], Glenda Mernaugh[3], Sidney Strickland[2], Roy Zent[3,4] and Peter D. Yurchenco[1,†]

SUMMARY

In order to understand the functions of laminins in the renal collecting system, the *Lamc1* gene was inactivated in the developing mouse ureteric bud (UB). Embryos bearing null alleles exhibited laminin deficiency prior to mesenchymal tubular induction and either failed to develop a UB with involution of the mesenchyme, or developed small kidneys with decreased proliferation and branching, delayed renal vesicle formation and postnatal emergence of a water transport deficit. Embryonic day 12.5 kidneys revealed an almost complete absence of basement membrane proteins and reduced levels of α6 integrin and FGF2. mRNA levels for fibroblast growth factor 2 (FGF2) and mediators of the GDNF/RET and WNT11 signaling pathway were also decreased. Furthermore, collecting duct cells derived from laminin-deficient kidneys and grown in collagen gels were found to proliferate and branch slowly. The laminin-deficient cells exhibited decreased activation of growth factor- and integrin-dependent pathways, whereas heparin lyase-treated and β1 integrin-null cells exhibited more selective decreases. Collectively, these data support a requirement of γ1 laminins for assembly of the collecting duct system basement membrane, in which immobilized ligands act as solid-phase agonists to promote branching morphogenesis, growth and water transport functions.

KEY WORDS: Kidney, Basement membrane, Heparan sulfates, Integrin, Growth, Diabetes insipidus, Mouse

INTRODUCTION

Metanephric kidney development commences when the Wolffian duct extends out to form the ureteric bud (UB) under the inductive influence of glial-derived neurotrophic factor (GDNF) (Shakya et al., 2005). The bud undergoes growth and branching to form the collecting ducts and induces the mesenchyme to condense and form epithelial vesicles that give rise to nephrons. A number of factors are involved in the mediating UB differentiation, including heparan sulfates, morphogens or growth factors that include GDNF and fibroblast growth factors (FGF), TGFβ family members and β1 integrins (Bates, 2007; Bullock et al., 1998; Bush et al., 2004; Steer et al., 2004; Wu et al., 2009; Zhang et al., 2009). The kidney basement membranes can be conceived as solid-phase agonists capable of mediating information to cells through interactions of these factors.

Laminins are heterotrimeric glycoproteins, most sharing a γ1 subunit, involved in basement membrane assembly and function (for a review, see Yurchenco, 2011). Inactivation of the *Lamc1* gene (γ1 subunit) in mice resulted in a failure of assembly of the embryonic plate basement membrane and Reichert's membrane, and developmental arrest (Smyth et al., 1999). Embryoid bodies, development of which mimics that of the peri-implantation embryo, required laminin for basement membrane assembly and epiblast polarization (Li et al., 2002; Murray and Edgar, 2000). Tissue-specific knockout of the gene in Schwann cells caused a reduction of endoneurial basement membranes, loss of myelination and increased apoptosis (Chen and Strickland, 2003; Yu et al., 2005).

Developing collecting system basement membranes share laminin γ1 and β1 subunits paired with the α1 or α5 subunit (Durbeej et al., 1996; Miner et al., 1997), making them ideal structures in which to define the role of these laminins in the morphogenesis of organs made of polarized epithelial cells. We therefore selectively inactivated the *Lamc1* gene in the kidney UB and its collecting duct derivatives by crossing the conditional knockout mouse with a cre mouse under the control of the *Hoxb7* promoter (Zhao et al., 2004). Inactivation of the laminin gene was found to cause a severe, yet time-limited, hypomorphic state. In some embryos, the UB failed to form, resulting in renal and ureteral agenesis. In others, the UB grew and branched slowly, resulting in small kidneys followed by hydronephrosis and diabetes insipidus. Exploration with cultured explants and collecting duct (CD) cells suggested that the growth defect results from both a loss of heparan sulfate-tethering of growth factors and reduced β1 integrin interactions acting through integrin, MAP kinase and receptor tyrosine kinase pathways.

MATERIALS AND METHODS

Targeted disruption of γ1 laminin in the developing collecting duct system

The *Lamc1* gene was inactivated in the UB by mating mice in which *Lamc1* exon-2 is flanked by lox-P sites (Chen and Strickland, 2003) with mice heterozygous for a *Hoxb7eGFPCre* transgene (Zhao et al., 2004) that express cre recombinase and GFP in the UB from embryonic day (E) 10.5. Mice homozygous for the lox-P flanked (fl, 'floxed') allele were maintained in both a C57Bl/6 and C57Bl/6-129SvEvTac backgrounds and the cre-recombinase mice were initially maintained in an FVBN/J background. Laminin-deficient ($Lamc1^{-/-Hoxb7}$) and littermate control ($Lamc1^{+/-Hoxb7}$ and $Lamc1^{+/fl}$) embryos and mice were generated by breeding males expressing the *Hoxb7eGFPcre* transgene and heterozygous

[1]Department of Pathology and Laboratory Medicine, Robert Wood Johnson Medical School, Piscataway, NJ 08854, USA. [2]Laboratory of Neurobiology and Genetics, Rockefeller University, New York, NY 10021, USA. [3]Division of Nephrology, Vanderbilt University, Nashville, TN 37232-2358, USA. [4]Department of Medicine, Veterans Affairs Hospital, Nashville, TN 37212-2637, USA.

*Present address: Fox Chase Cancer Center, 333 Cottman Ave., Philadelphia, PA 19111, USA
†Author for correspondence (yurchenc@umdnj.edu)

Accepted 10 August 2011

for the laminin floxed allele with *Lamc1*$^{fl/fl}$ females. *Hoxb7 cre* and floxed alleles were identified by PCR performed on genomic DNA from mice tails as described (Chen and Strickland, 2003; Zhao et al., 2004). All animal experiments were conducted according to institutional and national guidelines under an approved protocol.

Tissue preparation and immunohistology

Kidneys, adrenals, ureters and bladder were excised as a single block from newborn pups. Embryonic urogenital specimens were isolated at E10.5-12.5 (presence of a vaginal plug defined as E0.5) after maternal sacrifice. Whole-mount embryonic kidneys were incubated with primary antibodies (Table 1) at 4°C overnight.

For cryosections, kidneys at E12.5-14.5 were isolated, usually fixed in 3% paraformaldehyde (PFA) for 30 minutes at room temperature, embedded in OCT (Tissue-Tek, Elkhart, IN, USA), sectioned (5 μm thick) with a cryostat (Leica CM 1850) at –20°C and adhered to positively charged slides (Fisher). Sections were blocked with 1% bovine serum albumin (BSA) in phosphate-buffered saline (PBS) and then stained with primary antibodies. For staining with α6 integrin antibody (GoH3), kidneys were frozen in liquid nitrogen, sectioned, fixed in ice-cold methanol and blocked in 50 mM Tris-HCl containing 90 mM NaCl, 5% goat serum and 0.5% BSA. Detection of bound primary antibodies was accomplished with Alexa Fluor 647 goat anti-rabbit IgG and Alexa Fluor 488 anti-mouse IgG or anti-rat IgG secondary antibodies (Molecular Probes) at 1:100 dilution and counterstained with 2 μg/ml of the nuclear stain DAPI (4′-6-diamidino-2-phenylindole). Cover slips were mounted with SlowFade reagent (Molecular Probes, S2828) to inhibit photobleaching.

Microscopy

Embryonic tissues and slides were viewed by indirect immunofluorescence using an inverted microscope (model IX70; Olympus) fitted with an IX-FLA fluorescence attachment and a MicroMax 5-mHz CCD camera (Princeton Instruments) controlled by IP Lab 3.5 (Scanalytics).

For electron microscopy, kidneys were fixed in 0.5% gluteraldehyde and 0.2% tannic acid in PBS for 1 hour, washed with 0.1 M sodium cacodylate buffer, transferred to modified Karnovsky's fixative, post-fixed in 1% osmium tetroxide for 1 hour, dehydrated through ethanol and embedded in Epon/SPURR resin (EM Science). Semi-thin (1 μm) and thin sections (~90 nm) were cut with a diamond knife on a Leica model EMUC6 ultramicrotome. Semi-thin sections were stained with 1% Methylene Blue in 1% sodium borate and imaged using a Nikon Eclipse50 microscope. Thin sections were stained with saturated uranyl acetate followed by 0.2% lead citrate and imaged with a Philips CM-12 transmission electron microscope fitted with a digital camera (Hamamatsu ORCA-HR) controlled by AMT Image Capture software.

Table 1. Antibodies

Antibody	Species and type	Immunofluorescence	Immunoblot	Source or reference
Lm-111 [mouse Englebreth Holm-Swarm (EHS) laminin α1β1γ1 subunits], affinity purified	Rabbit polyclonal	1 μg/ml	–	Tsiper and Yurchenco, 2002
Lm-γ1 (γ1 laminin)	Mouse monoclonal (clone 2E8; mAb1920)	1:400	–	Millipore/Upstate
E4 (mouse Lm-111 fragment E4 consisting of Lmβ1LN-LEa), affinity purified	Rabbit polyclonal	5 μg/ml	–	Colognato et al., 1999
nidogen (mouse Nd-1), affinity purified	Rabbit polyclonal	10 μg/ml	–	Li et al., 2002
perlecan (mouse EHS), cross-absorbed	Rabbit polyclonal	2μg/ml	–	Handler et al., 1997
collagen-IV (mouse EHS α1,α2)	Rabbit polyclonal	1:100	–	Rockland, 600-401-106-05
agrin (LG domains)	Rabbit polyclonal	1:1000	–	Takako Sasaki (University of Erlangen, Germany)
collagen-XVIII (NC11)	Rabbit polyclonal	1:1000	–	Takako Sasaki
pan-cytokeratin	Mouse monoclonal	1:100	–	Sigma, c2562
α-dystroglycan (IIH6)	Mouse IgM monoclonal	1:100	–	Upstate, 05-593
E-cadherin	Rat monoclonal	1:100	–	Zymed, 13-1900
integrin α6 (GoH3), ascites	Rat monoclonal	1:200	–	Lydia Sorokin (University of Münster, Germany)
integrin α6 (GoH3), ascites	Rat monoclonal	1:100	–	Chemicon, mAb 1378
integrin β1	Rat monoclonal	1:100	–	Chemicon, mAb1997
FGF2	Mouse monoclonal	1:100	–	Upstate, 05-118
FGFR1	Rabbit polyclonal	1:100	–	Santa Cruz, sc-121
FGFR2	Rabbit polyclonal	1:100	–	Santa Cruz, sc-122
nephronectin	Rabbit polyclonal	1:100-1:200	–	Louis F. Reichardt (UCSF, CA, USA)
PAX2	Rabbit polyclonal	1:200	–	Zymed, 71-6000
AKT	Rabbit polyclonal	–	1:1000	Cell Signaling, 9272
phospho-AKT (pS473)	Rabbit polyclonal	–	1:1000	Cell Signaling, 9271
focal adhesion kinase (FAK)	Rabbit polyclonal	–	1:1000	Cell Signaling, 3285
phospho-FAK (pY925)	Rabbit polyclonal	–	1:1000	Cell Signaling, 3284
FGFR1	Rabbit polyclonal	–	1:1000	Cell Signaling, 3472
phospho-FGFR	Rabbit polyclonal	–	1:1000	Cell Signaling, 3471
Erk1/2	Rabbit polyclonal	–	1:1000	Cell Signaling, 9102
phospho-Erk1/2 (pT202,pY204)	Rabbit polyclonal	–	1:1000	Cell Signaling, 9101
paxillin	Rabbit polyclonal	–	1:1000	Cell Signaling, 2542
phospho-paxillin (pY118)	Rabbit polyclonal	–	1:1000	Cell Signaling, 2541
p38	Rabbit polyclonal	–	1:1000	Cell Signaling, 9212
phospho-p38 (pT180,pY182)	Rabbit polyclonal	–	1:1000	Cell Signaling, 9211

Organ and cell cultures

Whole-mount embryonic kidneys were cultured (37°C, 5% CO_2) on Transwell filters (Costar) within wells of a 24-well tissue culture dish containing Dulbecco's Modified Eagle Medium (DMEM, Gibco) supplemented with 10% fetal bovine serum (FBS) and antibiotics for up to 3 days. The GFP-positive fluorescent ureteric branches were photographed.

For collecting duct (CD) cell cultures, cells were isolated from *Lamc1*$^{fl/fl}$ mice as described (Husted et al., 1988). Kidneys were removed and rinsed in DMEM and Ham's F-12. Papillae were then dissected, minced to fine pieces, placed in 0.1% collagenase in Kreb's buffer for 2.5-3 hours and suspended in DMEM:F12 medium supplemented with 10% FBS and allowed to grow. These original cell populations were transformed with SV40 at passage three. The cells were then treated with adenoCre-GFP virus, cloned (GFP-positive cells) and expanded in culture. Deletion of *Lamc1* was verified by PCR genotyping. β1 integrin-deficient CD cells were prepared as described (Zhang et al., 2009). CD cells were cultured in a type I collagen (collagen-I; BD Biosciences) gel (1 mg/ml) supplemented with different concentrations of laminin-111 based on the method described by Chen et al. (Chen et al., 2004). CD cells (1.5×10^3) were suspended in 100 μl of collagen-I (1 mg/ml) containing 0.1 mg/ml of laminin-111 and cultured in 96-well dishes. After polymerization for 0.5 hours at 37°C, 100 μl of DMEM containing 20 mM HEPES (pH 7.2) and 10% FBS was added to the gels. CD cells were grown for 6-7 days in the presence of 10% fetal calf serum, serum separated into heparin-binding (HB+) and non-binding (HB–) fractions by heparin-affinity chromatography and serum-free medium containing the following growth factors (GFs): fibroblast growth factor 2 (FGF2, 10 ng/ml), GDNF (100 ng/ml), transforming growth factor-α (TGFα, 1 ng/ml), FGF10 (25 ng/ml), pleotrophin (PTN, 1 μg/ml), heparin-binding epidermal growth factor (HB-EGF, 5 ng/ml), hepatocyte growth factor (HGF, 50 ng/ml), and a mixture of the above factors.

Proliferation and apoptosis assays

Kidney cell proliferation was measured by injecting 0.2 ml of 20 mM 5-ethynyl-2′-deoxyuridine (EdU) intraperitoneally into pregnant females followed by embryonic harvest three hours later (Zeng et al., 2010). EdU incorporation was detected in frozen sections with the Click-iT EdU Alexa Fluor 594 imaging kit (Invitrogen, Carlsbad, CA, USA) and counterstained with DAPI to detect nuclei.

To measure CD cell proliferation within collagen gels (96-well plates), cells were incubated with 10 μM EdU for one hour, washed, fixed in 3.7% PFA for 15 minutes, permeabilized with 0.1% Triton X-100, reacted with Click-iT Alexa-594 dye-conjugate, and stained with DAPI. The fraction of cells undergoing DNA synthesis was determined following imaging by manual counts of Edu-positive and DAPI-stained nuclei.

For apoptosis, TUNEL was used to detect TdT-mediated dUTP incorporation into DNA ends using the DeadEnd Colorimetric Apoptosis Detection System (Promega). Tissues were permeabilized with proteinase K and post-fixed sections with 4% PFA in PBS. Incorporation of biotinylated nucleotide catalyzed by the TdT enzyme was carried out for 1 hour at 37°C. The incorporated biotinylated nucleotides were stained using streptavidin-conjugated horseradish peroxidase (HRP) with 3,3′-diaminobenzidine (DAB) as chromogen.

Immunoblotting

CD cells cultured in collagen gels were treated with 0.2 μg/ml bacterial collagenase I (Worthington) followed by centrifugation of the liberated cell clumps. Cells were lysed and extracted with Laemmli solubilizing buffer. Equal protein loads determined by Pierce BCA assay were electrophoresed by SDS-PAGE (6-10% gels, reducing conditions) and subsequently transferred to nitrocellulose membranes. Membranes were blocked in 3% BSA in PBS with 0.1% Tween 20, incubated with primary antibodies followed by appropriate HRP-conjugated secondary antibodies. Immunoreactive bands were detected using enhanced chemiluminescence (Thermo Scientific). Antibodies used were obtained from Cell Signaling (Table 1). The light emitted from the blots were imaged with a BioRad Gel Doc 2000 and analyzed using Quantity One software (BioRad). The numerical data were then subjected to statistical analysis (Student's *t*-test) with the program SigmaStat (v3.5) integrated into the graphing program SigmaPlot (v10).

Urine osmolality

Osmolality of urine collected from mice was measured by freezing-point determination using a Micro Osmometer (Advanced model 3MO Plus). For determination of vasopressin response, urine was collected immediately prior to and 3 hours after injection of arginine-vasopressin (200 ng/ml solution, 2 ng/gm body weight).

Quantitative real-time PCR analysis

RNA was isolated and stabilized from kidney with reagents provide by an RNeasy Plus Mini Kit (Qiagen). Real-time reverse-transcriptase polymerase chain reaction (qRT-PCR) was carried out to quantify transcripts encoding γ1 laminin, FGF7, FGF2, nephronectin, GDNF, RET, FGFR2, perlecan, nidogen 1, type IV collagen, WNT11 and WNT9B in embryonic kidneys, and aquaporin-2 (AQP2) and arginine vasopressin receptor 2 (AVPR2) in adult kidneys by using an ABI 7900 HT Sequence Detection System for measurement of the binding of fluorescence dye SYBR Green to double strand DNAs (DNA Core Facility). In order to normalize variations in mRNA extraction and cDNA synthesis, the expression of glyceraldehyde-3-phosphate dehydrogenase (GAPDH) was measured simultaneously. All primer sets were purchased from Qiagen. PCR reactions were set up in 96-well PCR tubes with each tube containing 60 ng mRNA mixed with 12.5 μl of 2× Quantitect SYBR Green RT-PCR Master Mix (Qiagen QuantiFast SYBR Green RT-PCR) and 0.3 μM primers. Triplicate aliquot reactions were carried out for each sample at 50°C for 10 minutes, initial activation at 95°C for 5 minutes followed by 40 cycles of denaturation at 95°C for 10 seconds and combined annealing/extension at 60°C for 30 seconds. A relative quantification method (Applied Biosystems 'Guide to Performing Relative Quantitation of Gene Expression Using Real-Time Quantitative PCR') was used to compare mRNA expression in which the C_T value (threshold cycle) was calculated ($\Delta C_T = CT_{sample} - CT_{GRPDH}$) as the mean of the triplicate samples. The difference between C_T values of samples for each target and mean C_T value of the reference for that target was then determined as $\Delta\Delta C_T$ (where $\Delta\Delta C_T = \Delta C_T$ mutant sample $- \Delta C_T$ control sample) and used to establish fold difference ($2^{-\Delta\Delta Ct}$).

RESULTS

Lamc1$^{-/-Hoxb7}$ embryonic kidneys are absent or small

Mice heterozygous for a *Hoxb7Cre-eGFP* transgene and floxed *Lamc1* were mated with mice homozygous for the floxed laminin gene. Recombination was verified by PCR as described in Materials and methods (see Fig. S1 in the supplementary material). Postnatal day (P) 0-1 pups with deficient UB laminin (*Lamc1*$^{-/-Hoxb7}$) either possessed small kidneys or lacked both kidneys and ureters with empty bladders when compared with littermate control (*Lamc1*$^{+/-Hoxb7}$ and *Lamc1*$^{fl/fl}$) animals (Fig. 1A-C). Mice without kidneys died shortly after birth. The defects were found in both females and males with no sex organ abnormalities. About one-third of mutant animals had absent kidneys and two-thirds had small kidneys (see Table S1 in the supplementary material).

Mice with small kidneys develop diabetes insipidus and hydronephrosis

Eleven laminin-deficient mice were examined for urinary defects starting at about 3 weeks of age when normal mice develop the ability to concentrate urine (Gattone et al., 1999). Eight of these mice (6/6 females and 2/5 males) produced large volumes of a dilute urine. Urine osmolality was noted to be lower in mutant mice compared with controls (Fig. 1D) and it did not respond to arginine-vasopressin like the normal littermates. Immunostaining of the collecting ducts using an antibody to the water channel protein aquaporin 2 revealed that the protein was less apically distributed and/or substantially decreased in overall staining in many of the collecting ducts of the laminin-deficient kidneys (Fig.

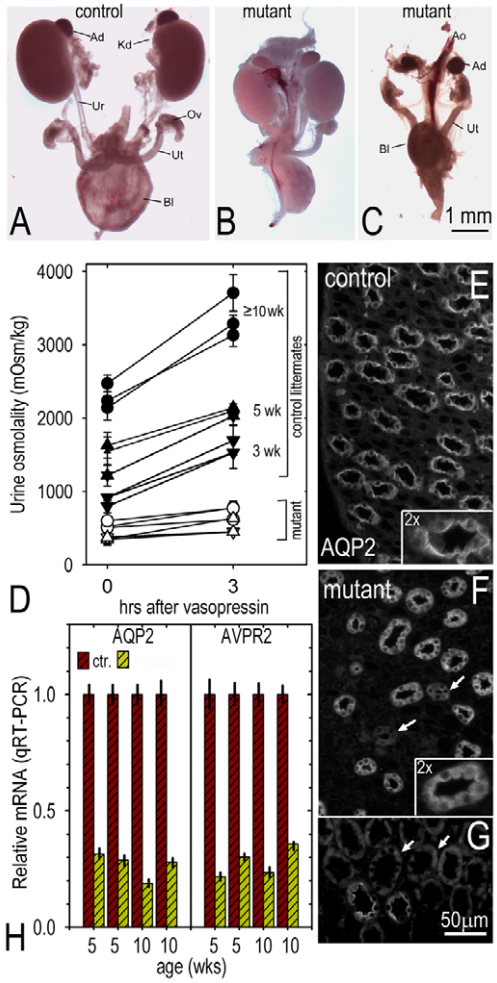

Fig. 1. Postnatal phenotypes. (**A-C**) Kidneys (Kd), adrenal glands (Ad), ureters (Ur), bladder (Bl), ovaries (Ov) and uterus (Ut) with portions of abdominal aorta (Ao) were dissected from newborn (P0-P1) heterozygous (A) and homozygous mutant (B,C) female pups. Mutant mice either had kidneys, both small with normal appearing ureters and bladder, or lacked both kidneys and ureters with empty bladders. (**D-H**) Postnatal urine concentration defect. (D) Urine osmolality (mean ± s.d. of three consecutive measurements per mouse) before and after vasopressin treatment of laminin-deficient (filled symbols) and control (open symbols) littermates at 3 weeks (inverted triangles), 5 weeks (triangles) and ≥10 weeks (circles) of age. (E-G) Aquaporin 2 immunostaining in adult (E) control and (F,G) laminin-deficient renal papillae (latter shown from two fields, one an overlapping composite; arrows indicate weakly stained collecting ducts). Collecting ducts from control papillae had bright apical distributions of aquaporin 2. Ducts from mutant papillae had an altered pan-intracellular distribution (arrows) of aquaporin 2 that was often reduced in intensity. (H) Quantitative RT-PCR determinations for the mRNAs encoding aquaporin 2 (AQP2) and the vasopressin 2 receptor (AVPR2) extracted from four control and four laminin-deficient kidneys.

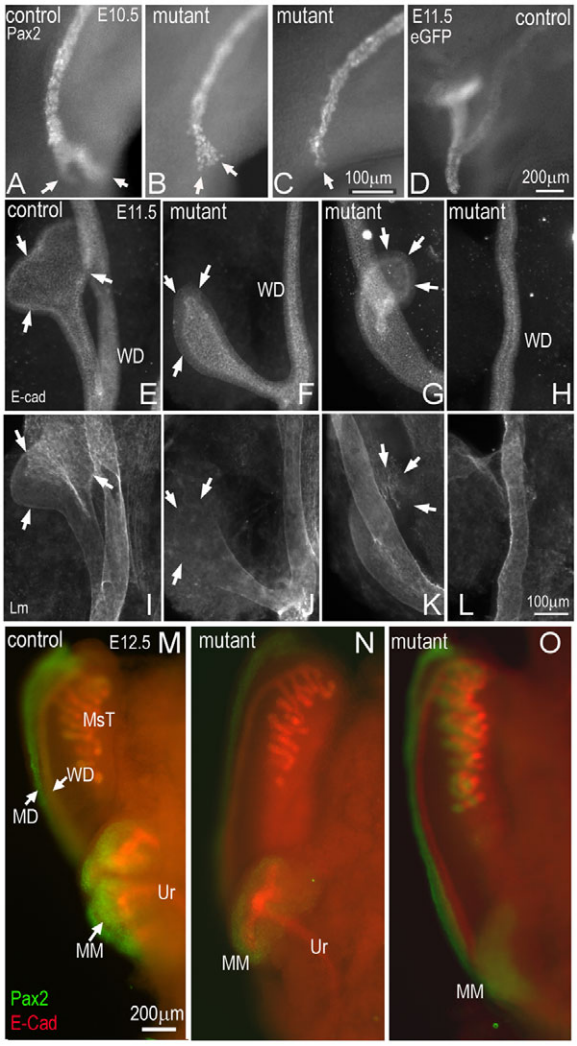

Fig. 2. Early UB development. (**A-C**) Immunofluorescence of the Wolffian duct (WD) of laminin-deficient (B,C) and control (A) mouse embryos at E10.5 stained with an antibody for PAX2 (caudal end shown). Ureteric and cloacal branches (arrows) are seen in the control embryos whereas single broadened or pointed tips are seen in the mutant embryos. (**D**) eGFP expression pattern at E11.5 in a control embryo. (**E-L**) E11.5 embryos were stained with antibodies for E-cadherin (E-cad) and laminin-111 (Lm) following removal of anterior structures. At E11.5, the control UB (E,I), seen branching from the Wolffian duct (WD), possessed two buds bifurcating from a common stalk. Mutant embryos possessed either a smaller unbranched bud or no branch at all. Laminin was detected over the surface (arrows) of the tips and stalk of wild-type UBs, but not the tips of mutant UBs. (**M-O**) Expression of PAX2 (green) and E-cadherin (red) at E12.5. Metanephric mesenchyme (MM) penetrated by a branching UB structure is seen in the control embryo (M). Mutant embryos possessed either a smaller rudimentary kidney (N) or an MM without UB penetration (O). Ur, ureter; MD, Müllerian duct; MsT, mesonephric tubules.

1E-G). Reduced expression of both the water channel protein aquaporin 2 and the vasopressin 2 receptor was confirmed in mutant mice relative to their control littermates by quantitative RT-PCR (Fig. 1H). The kidneys and ureters of mutant mice revealed dilated calyces without evidence for obstruction or dilation of the ureters, consistent with non-obstructive hydronephrosis (see Fig. S2 in the supplementary material).

Metanephric morphogenesis

To define the mechanisms of the developmental defects observed in the kidneys, embryos were examined between E10.5 and E12.5 (Fig. 2). In wild-type embryos, the caudal end of the Wolffian duct, detected at E10.5 with antibody to E-cadherin, was bifurcated into its ureteric bud (UB) and common nephric duct branches (Fig. 2A), whereas mutants exhibited either a broadened funnel-shaped tip

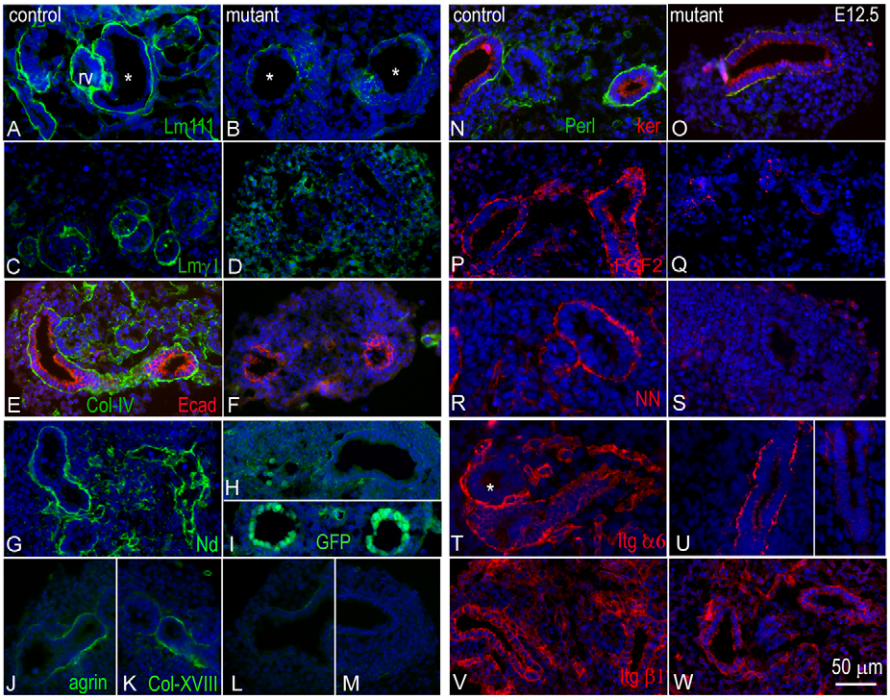

Fig. 3. Reduced basement membrane-zone components at E12.5. (**A-W**) Kidney sections from control (A,C,E,G,J,K,N,P,R,T,V) and mutant (B,D,F,H,I,L,M,O,Q,S,U,W) mouse embryos were immunostained with antibodies to laminin-111 (Lm111; A,B), γ1 laminin (Lmγ1; C,D), collagen IV (Col-IV; E,F), nidogen 1 (Nd; G,H), agrin (J,L), collagen XVIII (Col-XVIII; K,M), perlecan (Perl; N,O), FGF2 (P,Q), nephronectin (NN; R,S), α6 integrin (Itg α6; T,U), β1 integrin (Itg β1; V,W), E-cadherin (Ecad; E,F) and cytokeratin (ker; N,O), all counterstained with DAPI (blue). The basement membrane components α6 integrin, nephronectin and FGF2 were reduced in mutant kidneys. Antibodies to keratin and E-cadherin stained UB-derived epithelia of mutant kidneys, but not the renal vesicles (rv), which were seen only in control kidneys. Asterisks indicate UB branch lumens.

without bifurcation or a single narrow tip (Fig. 2B,C), suggesting that there was a smaller UB or no UB formed at this stage. GFP fluorescence was observed in the newly formed 'T-shaped' UB at the caudal end of the Wolffian duct by E11.5 (Fig. 2D) and remained strong in the developing ureter and ureteric branches in subsequent days. A single bifurcating UB coated with laminin (detected with polyclonal antibody; monoclonal antibody was insufficiently sensitive) was observed in control embryos at this stage (Fig. 2E,I). By contrast, mutant UBs were either small and unbranched with undetectable (Fig. 2F,G,J,K) or absent (Fig. 2H,L) laminin at the ureteric tip. By E12.5, control embryos possessed more than two ureteric branches, whereas null embryos possessed either a single bifurcation or no UB at all with a rudimentary blastema (Fig. 2M-O). The Wolffian duct, more rostral mesonephric tubular branches and Müllerian duct otherwise had similar appearances in control and mutant embryos. From E13.5 onwards, embryos either had kidneys with ureters or lacked kidneys and ureters altogether.

Defective basement membrane and epithelial polarization and delayed renal vesicle formation

Laminin-deficient and control littermate kidneys were examined at E12.5 by brightfield (semi-thin sections) and electron microscopy (see Fig. S3 in the supplementary material). Whereas littermate control kidneys possessed UBs with more than one order of branching and adjacent nests of condensed mesenchyme, the laminin-deficient kidneys exhibited a single branch without condensed mesenchyme (see Fig. S3A-D in the supplementary material). The ultrastructure of the laminin-deficient kidneys was one of flat disordered epithelia in the ampulla (identified based on its larger lumen and cuboidal cells) with basal as well as apical tight junctions and largely absent or greatly attenuated basement membranes (see Fig. S3E-K in the supplementary material). Some laminin-deficient kidneys lacked any epithelia at all. In these, apoptotic figures were abundant (see Fig. S3L in the supplementary material) as confirmed by TUNEL staining (see Fig. S3M-O in the supplementary material).

Reduced structural components and receptors at E12.5 prior to mesenchymal basement membrane formation

To compare basement membrane and other components at E12.5, kidneys were evaluated by immunostaining (Fig. 3). Renal vesicles (not reactive with cytokeratin or E-cadherin antibodies) were observed in control but not in laminin-deficient kidneys. Laminin-111 subunits, γ1 laminin and β1 laminin (not shown) subunits, nidogen 1 and type IV collagen, which were strongly detected in control ureteric bud/collecting duct and renal vesicle epithelial basement membranes, were either not detected or observed at very low levels in the laminin-deficient kidney epithelia. Similarly, the heparan sulfate proteoglycans (HSPGs) perlecan, agrin and type XVIII collagen were considerably reduced in laminin-deficient kidneys. FGF2, which was detected most prominently in the basement membrane zone of the UB branches as well as within mesenchyme, was reduced throughout the mutant kidney. Attempts to detect other heparin-binding growth factors, such as FGF7 and FGF10, were unsuccessful using commercially available antibodies. α6 integrin was low to nearly absent in ureteric branches; however, differences in β1 integrin were not detected. Immunostaining for α- and β-dystroglycan was very low in control and laminin-deficient sections (images not shown). Of note, dystroglycan-null kidneys generated through conditional knockout in the UB had no obvious defect (Jarad et al., 2011). Nephronectin, reported to trigger the release of glial-derived neurotrophic factor by ligating α8β1 integrin to induce penetration of the UB (Brandenberger et al., 2001; Linton et al., 2007), was reduced in laminin-deficient UB-derived basement membranes (Fig. 3R,S).

Components of the developing kidney were also evaluated by real-time quantitative reverse transcriptase (qRT) PCR and plotted as the ratio of laminin-deficient:control mRNA levels (Fig. 4). *Lamc1* mRNA was reduced to 28% of control levels. The remaining message might be due to incomplete gene inactivation (trace immunostaining for laminin was noted in the deficient kidneys) and/or to low endogenous mesenchymal expression. *Fgf2*,

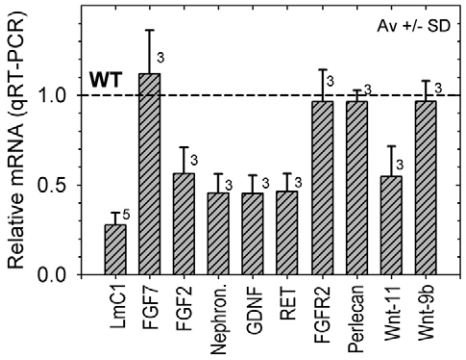

Fig. 4. Steady-state mRNA levels in E12.5 kidneys. RNA extracts were pooled from three embryos each and subjected to quantitative real-time reverse-transcriptase PCR (qRT-PCR) for genes encoding the indicated proteins (number of embryonic sets indicated at the top of the bars). In laminin-deficient samples, significant reductions were observed for mRNAs encoding γ1 laminin, FGF2, nephronectin, GDNF, RET and WNT11, but not FGF7, FGFR2, perlecan or WNT9B.

but not *Fgf7*, mRNA was reduced. Nephronectin, but not perlecan, type IV collagen or nidogen 1 (Fig. 4; data not shown) mRNAs were also reduced. *Gdnf*, its receptor *Ret*, and the UB factor *Wnt11* (but not *Wnt9b*) were reduced.

Increased laminin expression associated with induction of renal vesicles

Because laminins can diffuse from the site of secretion, it is possible that laminin derived from mesenchyme could assemble on UBs. This phenomenon might explain a gradual increase of laminin and other components detected in the developing collecting system as it matured. Initially, very low levels of punctate and pericellular γ1 laminin subunit were detected in E12.5 mesenchyme (Fig. 3). Furthermore, several laminin-deficient kidneys at stages later than E12.5 (where a laminin-immunostained condensed mesenchyme was present) demonstrated increased laminin staining in the UB, particularly that portion near to the laminin immunostained mesenchyme (Fig. 5). These increases, although below those of controls, were accompanied by increases in other basement membrane components, integrins and FGF2 (data not shown). Such findings support the interpretation that the laminin-deficient ureteric bud had gradually become invested with non-collecting duct laminins. By E14.5, a stage at which collecting ducts (keratin-stained), mesenchymally derived tubules (keratin-negative) and developing glomeruli were present in laminin-deficient and control littermates (Fig. 5B), γ1 laminin was detected in mutant collecting duct basement membranes, but at levels still below those of controls. The γ3 laminin subunit, absent at earlier stages of all kidneys, was found in the glomeruli of laminin-deficient and control kidneys, and to a lesser extent the collecting ducts, of all kidneys (Fig. 5B, inset). By birth, immunostaining intensities for γ1 laminin, laminin-111, perlecan, type IV collagen, α6 integrin and β1 integrin were similar in mutant and control kidneys (Fig. 5, lower panels; data not shown).

Reduced growth and branching of the UB

To characterize the later progression of changes of collecting duct system growth, GFP fluorescence was examined at E12.5-14.5 and at birth (Fig. 6A-H). Mutant kidneys were small and less branched relative to their control littermates at all developmental stages examined. Comparison of mutant and control branching revealed that

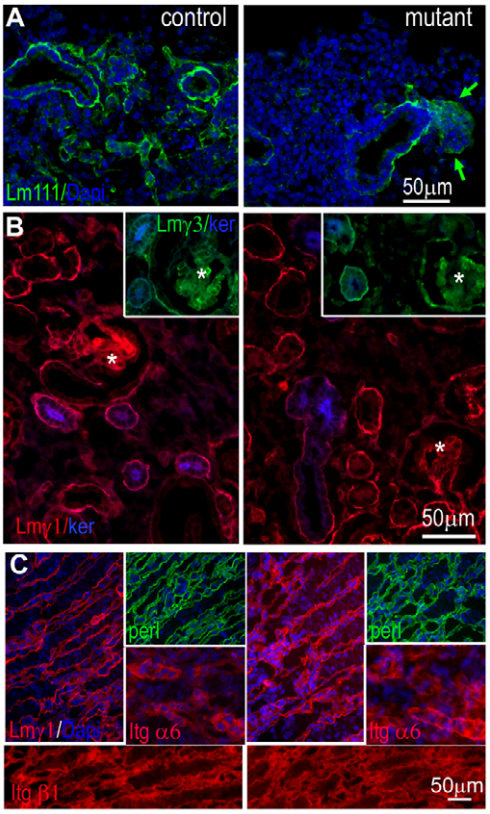

Fig. 5. Developmental age-related increase of collecting duct basement membrane components. (**A**) Appearance of laminin (Lm111) after the mesenchyme becomes condensed (green arrows) was associated with detection of increased laminin in the collecting duct branches of the laminin-deficient kidney. (**B**) At E14.5, expression of γ1 laminin was seen in the mesenchymal-transformed epithelia as well as in the collecting ducts. In null kidney, γ1 laminin (Lmγ1) immunostaining was strong in the basement membrane of mesenchymal-transformed epithelia (cytokeratin-negative) and weak in the null collecting ducts (cytokeratin-positive). Insets: γ3 laminin (Lmγ3) was detected in glomerular (asterisks) and tubular basement membranes of all kidneys. (**C**) Immunostaining intensities for γ1 laminin, perlecan (perl), α6 integrin (Itg α6) and β1 integrin (Itg β1) at P0 were of similar intensities in both normal and genetically laminin-deficient kidneys.

the defective kidneys lagged in terminal branch number by about one day of development from E12.5-14.5 (Fig. 6O). When E12.5 kidneys were cultured on filter membranes, mutant kidneys showed a similar delay in UB branching, consistent with the results in vivo (Fig. 6J-N). To determine whether proliferation and/or apoptosis contributed to slow UB growth, E12.5 embryos were labeled with EdU and TUNEL. Proliferation was significantly reduced in the UB branches (72% of control) and mesenchymal cells (67% of control) of laminin-deficient kidneys (Fig. 6Q-S). Increased apoptosis was confined to the blastema in the absence of UB penetration and was almost completely absent in control and small null kidneys by TUNEL assay (see Fig. S3 in the supplementary material).

Collecting duct cell growth and branching in vitro are dependent upon laminin, growth factors, heparan sulfate and β1 integrins

A consistent defect of laminin-deficient kidneys was the slow growth and reduced collecting duct branching. In order to address possible mechanisms underlying this defect in a relevant system that could

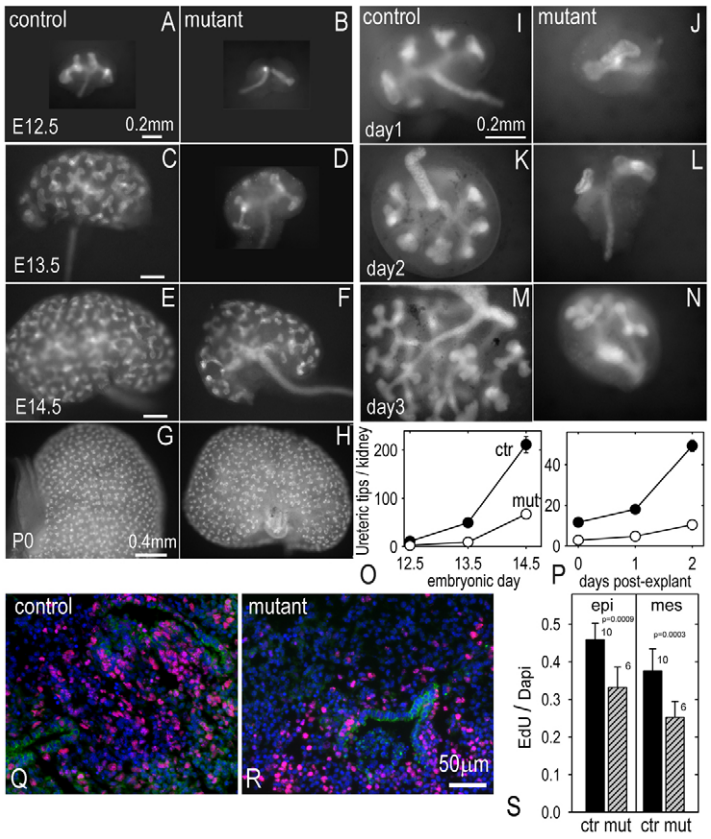

Fig. 6. Reduction of growth in laminin-deficient kidneys in mice and organ culture. (**A-N**) GFP fluorescence of control (A,C,E,G) and laminin-deficient (B,D,F,H) embryos were examined at the indicated times. In addition, kidneys at E12.5 were explanted and maintained in culture medium for two days at 37°C (I-N). (**O**,**P**) The number of bud tips was determined (n=3 kidneys for each) for the kidneys obtained from embryos at different stages (O) and from E12.5 kidneys grown in organ culture (P) and plotted as a function of stage or day of culturing (mean ± s.d.). (**Q-S**) Proliferation. Kidneys from ten control (Q) and six mutant (R) E12.5 embryos (three pregnancies) were labeled with EdU to compare DNA synthesis. The fraction of EdU-positive (red) DAPI-stained (blue) nuclei in UB-derived epithelia (defined by E-cadherin staining, green) and mesenchyme was determined by manual count (mean ± s.d.). Fewer UB-derived epithelia (P=0.009) and mesenchymal cells (P=0.003) underwent DNA replication in mutant kidneys compared with control kidneys.

provide sufficient cellular material for molecular analysis, laminin-deficient and β1 integrin-deficient CD cells grown within soft collagen I gels were evaluated (Fig. 7). Proliferation was assessed following labeling with EdU (Fig. 7A,B) and cell shape and branching was visualized by phalloidin-staining of F-actin (Fig. 7C). Cell elongation, branching and proliferation were observed to increase together with increasing concentrations of laminin-111. The decrease of HSPGs and loss of FGF2 in the laminin-deficient collecting ducts suggests that one basis for the growth defect was loss of growth factor-tethering by basement membrane heparan sulfates. In support of this possibility, treatment of CD cells with heparin lyases substantially reduced cell growth and branching. β1 integrin-null CD cells also grew and branched poorly. When the serum used to support the cells in culture was depleted of its heparin-binding components by heparin-affinity chromatography, cell proliferation and branching were reduced. This was restored by incubating with the heparin-binding (HB+) serum fraction. Several heparin-binding factors (GDNF, HB-EGF, FGF10, PTN, HGF, TGFα and FGF2) were also found to promote CD growth and branching in the absence of serum (data not shown).

To explore possible signaling contributions arising from growth factors and β1 integrins, CD lysates from laminin-deficient cells were immunoblotted and probed for phosphorylation of potential mediators (Fig. 8). Under the conditions used, perlecan, a basement membrane HSPG, was found to accumulate on CD cords following treatment with heparin lyases or chondroitinase ABC, but not in the absence of laminin as expected (Fig. 8A). Chondroitinase, which had no effect on growth of laminin-treated CD cells and did not alter phosphorylation of FGFR, ERK1/2 (MAPK3/MAPK1 – Mouse Genome Informatics), p38 MAP kinase (MAPK14 – Mouse Genome Informatics), AKT, paxillin or FAK (PTK2 – Mouse Genome Informatics) (data not shown), was used as a control. Reductions of FGFR, Erk1/2 and p38 MAP kinase, paxillin and FAK phosphorylation were observed in CD cells in the absence of added laminin. Following treatment with laminin and heparin lyase I+III, phosphorylation reductions in FGFR and downstream MAPK pathways (Erk1/2 and p38), but not in paxillin and FAK, were detected (Fig. 8B,C). Furthermore, when β1 integrin-null CD cells were grown for 6 days in collagen gels in the presence of laminin-111 and serum, significant decreases of phosphorylation of FAK, paxillin, ERK1/2, p38 and AKT, but only a slight (not significant) decrease of phosphorylation of FGFR1, were observed (see Fig. S4 in the supplementary material).

DISCUSSION

During metanephric development, different laminin α and β subunits join with the common γ1 subunit to generate different heterotrimers that populate the renal epithelial and vascular basement membranes (Miner et al., 1997). These subunits are important for kidney morphogenesis. For example, inactivation of the *Lama5* gene affects glomerulogenesis or causes renal agenesis (Miner and Li, 2000), whereas inactivation of the *Lamb2* gene, which is expressed later, affects glomerular filtration (Noakes et al., 1995). In this study, the role of γ1 laminins, which are effectively laminin-111 and laminin-511, was investigated in the context of UB development and function. The findings support the importance of these laminins for basement membrane assembly and reveal roles in collecting duct proliferation, which affects kidney size, and in emergence of postnatal competency to concentrate urine. In about a third of cases the UBs failed to protrude from the Wolffian duct to penetrate the blastema, leading to apoptosis of the renal mesenchyme and involution of the kidney. More frequently, the UB penetrated the blastema but grew and branched slowly. Very low levels of laminin were detected, arising from either a small fraction of UB cells that

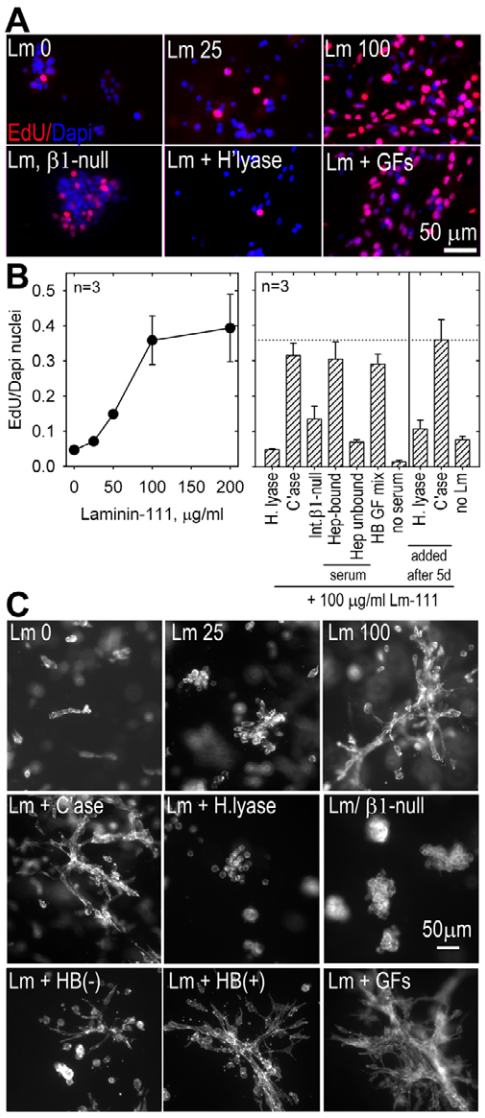

Fig. 7. Collecting duct cell proliferation and branching depends on laminin, β1 integrins and heparin-binding growth factors. CD cells were cultured in collagen I gels for 6 days. (**A**) Fluorescent images of CD cells supplemented with different concentrations of laminin-111 (Lm; 0, 25, 100 μg/ml), or with 100 μg/ml laminin-111 plus the following: β1 integrin-null CD cells (Lm, β1-null), heparin lyase I+III (Lm + H'lyase) or a mixture of heparin-binding growth factors (Lm + GFs). On day 6, cells were labeled with EdU for one hour, washed, fixed, reacted with Alexa Fluor 555 azide and counterstained with DAPI. (**B**) Proliferation (ratio of EdU:DAPI-positive nuclei) in response to increasing laminin-111 (left) and following treatment with 100 μg/ml laminin-111 plus heparin lyase I+III (H.lyase), chondroitinase ABC (C'ase), heparin-bound fraction of serum (Hep-bound), non-binding fraction of serum (Hep unbound), heparin-binding mixture of growth factors (HB GF mix), no serum, and β1 integrin-null (Int. β1-null) cells instead of laminin-null cells (no Lm) (right). Error bars represent mean ± s.d. (**C**) Growth and branching of laminin-null and integrin-null CD cells stained with rhodamine-phalloidin grown in the absence of laminin (Lm0) or with 25 μg/ml (Lm25), 100 μg/ml (Lm100) or 100 μg/ml Lm111 plus the following: chondroitinase (Lm+C'ase), heparin lyase I+III (Lm+H.lyase), β1 integrin-null CD cells (Lm/β1-null), heparin non-binding serum fraction [Lm + HB(–)], heparin-binding serum fraction (Lm + HB(+)] or growth factor mixture (Lm + GFs). CD proliferation and branching increased as the laminin concentration increased.

were not cre-inactivated, a low mesenchymal contribution or both. The bud tips, corresponding to the region found to possess the lowest level of detectable laminin at E11.5, developed a defect of polarization characterized by cuboidal epithelial cells with a disorganized distribution of tight junctions. Slow growth was due to decreased collecting duct proliferation and was accompanied by reduced mesenchymal proliferation. This was accompanied by a delay in formation of the renal vesicles.

A laminin-deficiency state was probably initiated at ~E10.5 when a defect in morphogenesis was first detected. At E12.5, the laminin-deficient kidneys had very little detectable nidogen 1, perlecan and type IV collagen with reduced α6 integrin subunit and FGF2, components normally found in the basement membrane zone. These changes probably reflect the known requirement of laminin expression for the assembly of other basement membrane structural components. Given unaltered transcription, the non-laminin components are presumably lost through diffusion and degradation. The laminin deficiency probably persists until the mesenchyme (independent of Hoxb7 activation) condenses, expresses laminins and forms the renal vesicle with an accompanying basement membrane (Ekblom, 1981; Ekblom et al., 1980; Klein et al., 1988). By birth, the levels of laminin and associated components could not be distinguished from controls. Although the basis for two fates of agenesis and small kidneys is unclear, it is possible that there is a bilaterally regulated laminin concentration threshold above which UB penetration is enabled.

Reduced UB and collecting duct growth

Basement membrane signals to cells are thought to be mediated through integrins and growth factors, the latter tethered to heparan sulfates and, in some cases, the core protein of perlecan (for reviews, see Iozzo, 2005; Yurchenco and Patton, 2009). As a γ1 laminin-deficiency in the developing collecting system caused an overall deficiency of basement membrane zone components and possible reduction in integrin and growth-factor signaling, the growth and branching defect might have resulted from a loss of these mediators. In support of an integrin role, β1 integrin-deficient kidneys were found to be small with reduced collecting duct branching (Zhang et al., 2009), but not as small as the kidneys examined in this study. β1 integrin-null CD cells exhibited decreased proliferation and branching. In support of a growth factor role, FGF2, a heparin-binding growth factor known to accumulate specifically in developing epithelial basement membranes (Evans et al., 2002), was reduced in the defective kidneys. Although it is unlikely that FGF2 is either the key or only reduced heparin-binding growth factor in developing kidney, it was the only heparin-binding factor that we were able to detect in control kidneys with available reagents. We suggest that a number of heparin-growth factors known to affect collecting duct growth (e.g. the heparin-binding factors and serum components we found to enhance CD proliferation and branching) are similarly reduced in laminin-deficiency because of the loss of heparan-sulfated perlecan, agrin and type XVIII collagen. Furthermore, the conclusion that a dual integrin and growth factor signaling reduction probably occurs with loss of laminin expression was supported by the finding that phosphorylation of FGFR1, mediators of integrin signaling and MAP kinase pathway mediators (common to both pathways) were all reduced in laminin-deficient CD cells.

A number of studies have revealed the importance of heparan sulfates and heparin-binding growth factors in the proliferation, branching and differentiation of the UB (Davies et al., 1995; Steer et al., 2004; Bullock et al., 1998). Targeted ablation of FGFR2 in

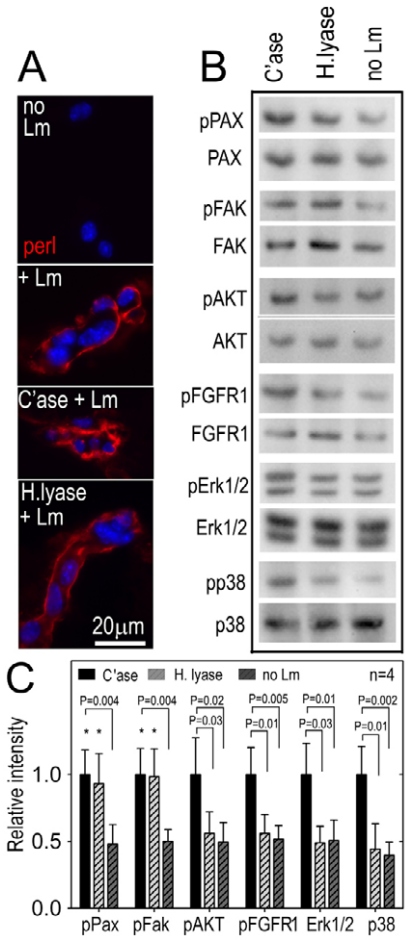

Fig. 8. Reduced growth factor- and integrin-dependent signaling in laminin-deficient and heparin lyase-treated collecting duct cells. (**A**) Cells growth without laminin (no Lm) or with laminin-111 (100 μg/ml) alone (+Lm) or with either chondroitinase ABC (C′ase + Lm) or heparin lyase I+III (H.lyase + Lm) added after 5 days. Cells were stained with a perlecan-specific antibody (perl, red) and counterstained with DAPI (blue). Accumulation of the endogenous component into linear basement membrane patterns was detected after laminin treatments. (**B**,**C**) Western blots of lysates from CD cultures with laminin-111 (100 μg/ml) without or with chondroitinase-ABC or heparin lyase I + III. Heparin lyase decreased growth factor and integrin signaling pathways (paired asterisks, $P>0.05$).

the developing UB was found to cause aberrant UB branching and reduced proliferation (Zhao et al., 2004), and kidneys null for the heparin-binding growth factor FGF7 were small due to reduced UB growth (Qiao et al., 1999). FGF2, which binds strongly to heparin, accumulates in developing basement membranes (Evans et al., 2002) and was detected at reduced levels in the mutant kidneys. Furthermore, FGF activation of its receptor tyrosine kinase receptors is dependent upon formation of a receptor-FGF-heparan sulfate complex (Schlessinger et al., 2000). Although the in vitro analysis does not preclude a contribution of heparan sulfate arising from cell surfaces rather than from basement membranes, the mouse kidney data argue for a unique basement membrane-HSPG-specific role in this regard. Given the mouse findings, it was thought that the observed effects on the growth of CD cells would depend upon signaling pathways associated with both integrins and receptor tyrosine kinases. This expectation was supported by the observation that laminin deficiency, unlike β1 integrin- and heparan sulfate deficiencies, resulted in significantly reduced phosphorylation of mediators of both β1 integrin (by FAK and paxillin) and the FGF receptor (by auto-phosphorylation), as well as the MAP-kinase pathway, a common pathway downstream of both (for a review, see Rozengurt, 2007).

Other basement membrane zone factors were altered as well. Nephronectin, a protein expressed and secreted by the UB and its branches, was not incorporated into collecting system basement membranes in the absence of γ1 laminin expression. Its mRNA was also reduced. Genetic ablation of the nephronectin gene was found to frequently result in unilateral or bilateral renal agenesis, with evidence that nephronectin normally stimulates GDNF expression by ligating its cognate α8β1 integrin (Brandenberger et al., 2001; Linton et al., 2007). The absence of this component might have contributed to defective UB penetration. It also could be that reduced GDNF caused a partial reduction of nephronectin transcription independent of a failure of nephronectin recruitment into the UB basement membrane. Furthermore, WNT11, a promoter of branching morphogenesis expressed at the tip of the ureteric bud, might be reduced as a consequence of reduced RET (Majumdar et al., 2003). However, the bases for reduced transcription of the RET and nephronectin are unclear.

Postnatal development of a urine-concentration defect

Mice with small kidneys were often unable to concentrate urine, reflecting a water transport defect resulting from reduced expression of the vasopressin receptor and aquaporin 2 transporter. An increase in the size of the cavity of the renal pelvis, thinning of the medulla and mild dilations of the proximal tubules without evidence of anatomical obstruction accompanied the defect. The histological changes might have resulted from increased outflow volume and pressure. Similar morphological changes were reported to develop in the kidneys of mice with dilute voluminous urine following inactivation of the gene for aquaporin 2 (Verkman, 2006; Yang et al., 2001). Furthermore, a similar urine concentration defect with decreased vasopressin receptor and aquaporin 2 was observed in mice following HoxB7-directed inactivation of the β1 integrin subunit (Wu et al., 2009). These findings suggest that development of a vasopressin-responsive water transport system requires β1 integrin ligation of the basement membrane. However, because in our study laminin and integrin levels were normal by birth, it is likely that the reduced expression resulted from a laminin- and integrin-dependent embryonic alteration of the collecting duct system. This might reflect an early cell fate change.

In conclusion, the findings reveal that a reduction of laminin results in a general failure of basement membrane assembly. The consequences of this structural loss supports a model of the basement membrane acting as a solid-phase agonist through two mechanistic pathways: structurally intrinsic integrin-binding ligands generated by the collecting system and basement membrane heparan sulfate-tethered growth factors provided by either the collecting system or mesenchyme, together acting to affect growth and branching. A requirement for the γ1 laminin subunit for proliferation has also been seen in developing Schwann cells (Yu et al., 2005; Yin et al., 2000). Finally, the evidence points to an embryonic basement membrane-β1 integrin interaction that is required for later maturation of a vasopressin-regulated water transport system.

Acknowledgements

We thank Carlton M. Bates (Children's Hospital of Pittsburgh of UPMC) for providing the Hoxb7GFP-cre mice for the study and for his helpful suggestions. We also thank Raj Patel (Electron Microscopy Service, Robert W. Johnson

Medical School) for preparing EM sections; Evan Cadoff and Peter S. Amenta (Robert Wood Johnson Medical School) for facilitating the analysis of urine osmolality and assistance in review of histology, respectively; and Takako Sasaki (University of Erlangen, Germany), Lydia Sorokin (University of Münster, Germany) and Louis Reichardt (University of California San Francisco) for antibodies.

Funding
This study was supported by grants from the National Institutes of Health (R37-DK36425 to P.D.Y.; R01-DK065123, R01-DK075594 and R01-DK65123 to R.Z.). It was also supported by the Foundation of UMDNJ (D.-H.Y.), an AHA established investigator award, merit award from the Department of Veterans Affairs, and George O'Brien Center Grant (R.Z.). Deposited in PMC for release after 12 months.

Competing interests statement
The authors declare no competing financial interests.

Supplementary material
Supplementary material for this article is available at
http://dev.biologists.org/lookup/suppl/doi:10.1242/dev.071266/-/DC1

References
Bates, C. M. (2007). Role of fibroblast growth factor receptor signaling in kidney development. *Pediatr. Nephrol.* **22**, 343-349.
Brandenberger, R., Schmidt, A., Linton, J., Wang, D., Backus, C., Denda, S., Muller, U. and Reichardt, L. F. (2001). Identification and characterization of a novel extracellular matrix protein nephronectin that is associated with integrin alpha8beta1 in the embryonic kidney. *J. Cell Biol.* **154**, 447-458.
Bullock, S. L., Fletcher, J. M., Beddington, R. S. and Wilson, V. A. (1998). Renal agenesis in mice homozygous for a gene trap mutation in the gene encoding heparan sulfate 2-sulfotransferase. *Genes Dev.* **12**, 1894-1906.
Bush, K. T., Sakurai, H., Steer, D. L., Leonard, M. O., Sampogna, R. V., Meyer, T. N., Schwesinger, C., Qiao, J. and Nigam, S. K. (2004). TGF-beta superfamily members modulate growth, branching, shaping, and patterning of the ureteric bud. *Dev. Biol.* **266**, 285-298.
Chen, D., Roberts, R., Pohl, M., Nigam, S., Kreidberg, J., Wang, Z., Heino, J., Ivaska, J., Coffa, S., Harris, R. C. et al. (2004). Differential expression of collagen- and laminin-binding integrins mediates ureteric bud and inner medullary collecting duct cell tubulogenesis. *Am. J. Physiol. Renal Physiol.* **287**, F602-F611.
Chen, Z. L. and Strickland, S. (2003). Laminin gamma1 is critical for Schwann cell differentiation, axon myelination, and regeneration in the peripheral nerve. *J. Cell Biol.* **163**, 889-899.
Colognato, H., Winkelmann, D. A. and Yurchenco, P. D. (1999). Laminin polymerization induces a receptor-cytoskeleton network. *J. Cell Biol.* **145**, 619-631.
Davies, J., Lyon, M., Gallagher, J. and Garrod, D. (1995). Sulphated proteoglycan is required for collecting duct growth and branching but not nephron formation during kidney development. *Development* **121**, 1507-1517.
Durbeej, M., Fecker, L., Hjalt, T., Zhang, H. Y., Salmivirta, K., Klein, G., Timpl, R., Sorokin, L., Ebendal, T., Ekblom, P. et al. (1996). Expression of laminin alpha 1, alpha 5 and beta 2 chains during embryogenesis of the kidney and vasculature. *Matrix Biol.* **15**, 397-413.
Ekblom, P. (1981). Formation of basement membranes in the embryonic kidney: an immunohistological study. *J. Cell Biol.* **91**, 1-10.
Ekblom, P., Alitalo, K., Vaheri, A., Timpl, R. and Saxen, L. (1980). Induction of a basement membrane glycoprotein in embryonic kidney: possible role of laminin in morphogenesis. *Proc. Natl. Acad. Sci. USA* **77**, 485-489.
Evans, M. J., Fanucchi, M. V., Van Winkle, L. S., Baker, G. L., Murphy, A. E., Nishio, S. J., Sannes, P. L. and Plopper, C. G. (2002). Fibroblast growth factor-2 during postnatal development of the tracheal basement membrane zone. *Am. J. Physiol. Lung Cell Mol. Physiol.* **283**, L1263-L1270.
Gattone, V. H., 2nd, Maser, R. L., Tian, C., Rosenberg, J. M. and Branden, M. G. (1999). Developmental expression of urine concentration-associated genes and their altered expression in murine infantile-type polycystic kidney disease. *Dev. Genet.* **24**, 309-318.
Handler, M., Yurchenco, P. D. and Iozzo, R. V. (1997). Developmental expression of perlecan during murine embryogenesis. *Dev. Dyn.* **210**, 130-145.
Husted, R. F., Hayashi, M. and Stokes, J. B. (1988). Characteristics of papillary collecting duct cells in primary culture. *Am. J. Physiol.* **255**, F1160-F1169.
Iozzo, R. V. (2005). Basement membrane proteoglycans: from cellar to ceiling. *Nat. Rev. Mol. Cell Biol.* **6**, 646-656.
Jarad, G., Pippin, J. W., Shankland, S. J., Kreidberg, J. A. and Miner, J. H. (2011). Dystroglycan does not contribute significantly to kidney development or function, in health or after injury. *Am. J. Physiol. Renal Physiol.* **300**, F811-F820.
Klein, G., Langegger, M., Timpl, R. and Ekblom, P. (1988). Role of laminin A chain in the development of epithelial cell polarity. *Cell* **55**, 331-341.
Li, S., Harrison, D., Carbonetto, S., Fassler, R., Smyth, N., Edgar, D. and Yurchenco, P. D. (2002). Matrix assembly, regulation, and survival functions of laminin and its receptors in embryonic stem cell differentiation. *J. Cell Biol.* **157**, 1279-1290.
Linton, J. M., Martin, G. R. and Reichardt, L. F. (2007). The ECM protein nephronectin promotes kidney development via integrin alpha8beta1-mediated stimulation of Gdnf expression. *Development* **134**, 2501-2509.
Majumdar, A., Vainio, S., Kispert, A., McMahon, J. and McMahon, A. P. (2003). Wnt11 and Ret/Gdnf pathways cooperate in regulating ureteric branching during metanephric kidney development. *Development* **130**, 3175-3185.
Miner, J. H. and Li, C. (2000). Defective glomerulogenesis in the absence of laminin alpha5 demonstrates a developmental role for the kidney glomerular basement membrane. *Dev. Biol.* **217**, 278-289.
Miner, J. H., Patton, B. L., Lentz, S. I., Gilbert, D. J., Snider, W. D., Jenkins, N. A., Copeland, N. G. and Sanes, J. R. (1997). The laminin alpha chains: expression, developmental transitions, and chromosomal locations of alpha1-5, identification of heterotrimeric laminins 8-11, and cloning of a novel alpha3 isoform. *J. Cell Biol.* **137**, 685-701.
Murray, P. and Edgar, D. (2000). Regulation of programmed cell death by basement membranes in embryonic development. *J. Cell Biol.* **150**, 1215-1221.
Noakes, P. G., Miner, J. H., Gautam, M., Cunningham, J. M., Sanes, J. R. and Merlie, J. P. (1995). The renal glomerulus of mice lacking s-laminin/laminin beta 2, nephrosis despite molecular compensation by laminin beta 1. *Nat. Genet.* **10**, 400-406.
Qiao, J., Uzzo, R., Obara-Ishihara, T., Degenstein, L., Fuchs, E. and Herzlinger, D. (1999). FGF-7 modulates ureteric bud growth and nephron number in the developing kidney. *Development* **126**, 547-554.
Rozengurt, E. (2007). Mitogenic signaling pathways induced by G protein-coupled receptors. *J. Cell. Physiol.* **213**, 589-602.
Schlessinger, J., Plotnikov, A. N., Ibrahimi, O. A., Eliseenkova, A. V., Yeh, B. K., Yayon, A., Linhardt, R. J. and Mohammadi, M. (2000). Crystal structure of a ternary FGF-FGFR-heparin complex reveals a dual role for heparin in FGFR binding and dimerization. *Mol. Cell* **6**, 743-750.
Shakya, R., Jho, E. H., Kotka, P., Wu, Z., Kholodilov, N., Burke, R., D'Agati, V. and Costantini, F. (2005). The role of GDNF in patterning the excretory system. *Dev. Biol.* **283**, 70-84.
Smyth, N., Vatansever, H. S., Murray, P., Meyer, M., Frie, C., Paulsson, M. and Edgar, D. (1999). Absence of basement membranes after targeting the LAMC1 gene results in embryonic lethality due to failure of endoderm differentiation. *J. Cell Biol.* **144**, 151-160.
Steer, D. L., Shah, M. M., Bush, K. T., Stuart, R. O., Sampogna, R. V., Meyer, T. N., Schwesinger, C., Bai, X., Esko, J. D. and Nigam, S. K. (2004). Regulation of ureteric bud branching morphogenesis by sulfated proteoglycans in the developing kidney. *Dev. Biol.* **272**, 310-327.
Tsiper, M. V. and Yurchenco, P. D. (2002). Laminin assembles into separate basement membrane and fibrillar matrices in Schwann cells. *J. Cell Sci.* **115**, 1005-1015.
Verkman, A. S. (2006). Roles of aquaporins in kidney revealed by transgenic mice. *Semin. Nephrol.* **26**, 200-208.
Wu, W., Kitamura, S., Truong, D. M., Rieg, T., Vallon, V., Sakurai, H., Bush, K. T., Vera, D. R., Ross, R. S. and Nigam, S. K. (2009). Beta1-integrin is required for kidney collecting duct morphogenesis and maintenance of renal function. *Am. J. Physiol. Renal Physiol.* **297**, F210-F217.
Yang, B., Ma, T. and Verkman, A. S. (2001). Erythrocyte water permeability and renal function in double knockout mice lacking aquaporin-1 and aquaporin-3. *J. Biol. Chem.* **276**, 624-628.
Yin, X., Kidd, G. J., Wrabetz, L., Feltri, M. L., Messing, A. and Trapp, B. D. (2000). Schwann cell myelination requires timely and precise targeting of P(0) protein. *J. Cell Biol.* **148**, 1009-1020.
Yu, W. M., Feltri, M. L., Wrabetz, L., Strickland, S. and Chen, Z. L. (2005). Schwann cell-specific ablation of laminin gamma1 causes apoptosis and prevents proliferation. *J. Neurosci.* **25**, 4463-4472.
Yurchenco, P. D. (2011). Basement membranes: cell scaffoldings and signaling platforms. *Cold Spring Harb. Perspect. Biol.* **3**, a004911.
Yurchenco, P. D. and Patton, B. L. (2009). Developmental and pathogenic mechanisms of basement membrane assembly. *Curr. Pharm. Des.* **15**, 1277-1294.
Zeng, C., Pan, F., Jones, L. A., Lim, M. M., Griffin, E. A., Sheline, Y. I., Mintun, M. A., Holtzman, D. M. and Mach, R. H. (2010). Evaluation of 5-ethynyl-2'-deoxyuridine staining as a sensitive and reliable method for studying cell proliferation in the adult nervous system. *Brain Res.* **1319**, 21-32.
Zhang, X., Mernaugh, G., Yang, D. H., Gewin, L., Srichai, M. B., Harris, R. C., Iturregui, J. M., Nelson, R. D., Kohan, D. E., Abrahamson, D. et al. (2009). Beta1 integrin is necessary for ureteric bud branching morphogenesis and maintenance of collecting duct structural integrity. *Development* **136**, 3357-3366.
Zhao, H., Kegg, H., Grady, S., Truong, H. T., Robinson, M. L., Baum, M. and Bates, C. M. (2004). Role of fibroblast growth factor receptors 1 and 2 in the ureteric bud. *Dev. Biol.* **276**, 403-415.